

# Tyrosine 162 of the Photosynthetic Reaction Center L-Subunit Plays a Critical Role in the Cytochrome $c_2$ Mediated Rereduction of the Photooxidized Bacteriochlorophyll Dimer in *Rhodobacter sphaeroides*. 1. Site-Directed Mutagenesis and Initial Characterization

J. W. Farchaus,<sup>†</sup> J. Wachtveitl, P. Mathis,<sup>§</sup> and D. Oesterhelt\*

Department of Membrane Biochemistry, Max Planck Institute for Biochemistry,  
am Klopferspitz 18a, 82143 Martinsried, Germany

Received April 15, 1993; Revised Manuscript Received July 20, 1993\*

**ABSTRACT:** Five site-directed mutants were engineered to substitute phenylalanine, serine, leucine, methionine, and glycine for tyrosine residue 162 of the *pufL* gene in *Rhodobacter (R.) sphaeroides*. Each of the mutations and the wild-type (WT) genes was expressed in the *R. sphaeroides puf* deletion strain PUFΔLMX21/3. Initial characterization revealed that all of the mutants were photoheterotrophically competent but that L162G and L162S were impaired. The amounts of mutant reaction centers expressed, the spectral characteristics, and the rates of intraprotein electron transfer and turnover were similar to the values obtained for WT. Kinetic measurements of photooxidized special pair rereduction mediated by the physiological donor cytochrome  $c_2$  in intact chemoheterotrophically grown cells revealed that the fast phase was abolished in all mutants and that the overall kinetics of rereduction was drastically slowed. It is concluded that L162Y plays a vital role in facilitating the rapid rereduction of the photooxidized bacteriochlorophyll dimer in *R. sphaeroides*.

The purple non-sulfur bacterium *Rhodobacter (R.) sphaeroides* is capable of growth by utilizing a light-driven, cyclic electron-transport pathway. The pathway is composed of two intrinsic membrane complexes: the reaction center (RC)<sup>1</sup> and the cytochrome  $bc_1$  complex. Cytochrome (cyt)  $c_2$ , which is located in the periplasm, and a pool of ubiquinone, thought to diffuse freely in the hydrophobic domain of the membrane, complete the cycle.

The RC is composed of three polypeptide subunits, H, L, and M. Four bacteriochlorophyll (bchl)  $a$  molecules, two bacteriopheophytin (bphe)  $a$  molecules, two ubiquinones, one carotenoid, and one non-heme iron are bound to the L- and M-subunits. A striking feature of the RC is that the chromophores as well as the L- and M-subunits are arranged with approximate  $C_2$  symmetry (Deisenhofer et al., 1985; Michel et al., 1986a; Allen et al., 1987). Due to unknown reasons, electron transfer proceeds selectively over one of the branches defined by the  $C_2$  symmetry axis. This axis runs from the non-heme iron on the cytoplasmic surface of the RC to a dimer of bchl  $a$  molecules located on the periplasmic side. The primary electron-transfer events begin when this dimer (P) is driven to an excited state ( $P^*$ ) by the absorption of light energy. The reversible photooxidation of this dimer ( $P^+$ ) ultimately results in the transfer of an electron to the bphe  $a$  on the L-branch of the RC in some 3.5 ps (Woodbury et al., 1985; Breton et al., 1988; Holzapfel et al., 1989). Evidence now exists to suggest that this electron transfer proceeds via

the monomeric "accessory" bchl  $a$  located between P and the bphe  $a$  (Holzapfel et al., 1990). The electron passes from the reduced bphe  $a$  to the primary quinone species,  $Q_A$ , in 200 ps (Rockley et al., 1975; Kaufmann et al., 1976) and finally ends up on the secondary quinone,  $Q_B$ . The charge separation is stabilized by the rereduction of the photooxidized  $P^+$  by cyt  $c_2$ . A second charge separation results in the reduction and protonation of  $Q_B^-$  to form the quinol  $Q_BH_2$ , whose release from the RC is the rate-limiting step in RC turnover with a half-time of 5 ms (Wraight, 1979). Cyclic electron flow is completed by the cyt  $bc_1$  complex utilizing the reduced quinol and oxidized cyt  $c_2$  as the electron donor and acceptor, respectively.

Analysis of the kinetics of electron transfer from cyt  $c_2$  to the photooxidized  $P^+$  in *R. sphaeroides* revealed that the process was multiphasic. A kinetic model was subsequently developed which adequately described the complex kinetics in terms of three distinct phases (Overfield et al., 1979): a fast first-order phase with a half-time in the microseconds range which has been assigned to an electron transfer from a cyt bound to a favorable "proximal" site on the RC; a slower 100–200- $\mu$ s first-order phase due to the reaction of a cyt bound at an unfavorable "distal" site; and a second-order phase observed under high ionic strength conditions or low cyt concentrations that is attributed to unbound cyt.

The molecular details of the RC and cyt structure–function relationship required for this electron-transfer process remain unclear. The crystallization of the RCs from *Rhodospseudomonas (Rps.) viridis* (reviewed in Deisenhofer and Michel (1989)) and *R. sphaeroides* (Rees et al., 1989; El-Kabbani et al., 1991) has added greatly to the understanding of this relationship and, specifically, allowed a systematic probing of individual amino acid residues as a means of probing their possible roles (Gray et al., 1990; Coleman & Youvan, 1990) in facilitating intra- or intermolecular electron-transfer processes. In the work described in this article, we have investigated the role of tyrosine L162 in docking and electron

\* Author to whom correspondence should be addressed.

<sup>†</sup> Bacteriology Division, United States Army Research Institute for Infectious Diseases, Fort Detrick, Frederick, MD 21701–5011.

<sup>§</sup> Section de Bioénergétique, Département de Biologie Cellulaire et Moléculaire, CEN Saclay, 91191 Gif-sur-Yvette Cedex, France.

• Abstract published in *Advance ACS Abstracts*, September 15, 1993.

<sup>1</sup> Abbreviations: bchl, bacteriochlorophyll; bphe, bacteriopheophytin; CFU, colony-forming unit; cyt, cytochrome; LDAO, *N,N*-dimethyldodecylamine *N*-oxide; OG, *n*-octyl  $\beta$ -D-glucopyranoside; P, primary donor (bacteriochlorophyll dimer); *R.*, *Rhodobacter*; RC, reaction center; *Rps.*, *Rhodospseudomonas*; UQ<sub>0</sub>, 2,3-dimethoxy-5-methylbenzoquinone; WT, wild type.

transfer from the cyt heme to P<sup>+</sup> in *R. sphaeroides*. We provide evidence that substitution of F, L, M, S, or G for L162Y resulted in a drastic reduction of the *in vivo* kinetics of P<sup>+</sup> rereduction by cyt *c*<sub>2</sub> without altering the absorption properties of the RC or other steps in intramolecular electron transfer within the RC. The results described here and in the following article indicate that L162Y is required for a fast and efficient interprotein electron transfer. A preliminary report on this work was published elsewhere (Farchaus et al., 1990).

## MATERIALS AND METHODS

**Bacterial Strains and Growth.** WT strain *R. sphaeroides* ATCC 17023 was obtained from the Deutsche Sammlung für Mikroorganismen (Göttingen, Germany). The neurosporene accumulating *R. sphaeroides* *pufLMX* deletion strain PUFΔLMX21/3 used in these studies was described previously (Farchaus & Oesterheld, 1989). In order to maximize the reproducibility of culture growth conditions for large-scale fermentations, the strains harboring *pufL* mutations on pRK404 were first streaked onto fresh Sistrom's (Sistrom, 1960) minimal medium (SMM)/kanamycin (25 μg/mL)/tetracycline (10 μg/mL) plates and cultured overnight at 30 °C in complete darkness. Cells from these plates were then inoculated into Erlenmeyer flasks filled to 50% of the total volume with SMM supplemented with kanamycin (25 μg/mL), tetracycline (2 μg/mL), and 0.2% (w/v) casamino acids (Difco, Detroit, MI). The cultures were incubated in darkness at 30 °C and 100 rpm overnight on a gyratory shaker with a displacement radius of 2.5 cm. The cultures were then added to 500 mL of the same medium and further subcultured under the same conditions until the early stationary phase [typically (1–1.2) × 10<sup>9</sup> CFU/mL]. The entire culture was then added to a 10-L B. Braun Biostat-E 880 fermentor (B. Braun GmbH, Melsungen, Germany) filled to a final working volume of 10 L with the same medium. The fermentor agitation was set at 100 rpm, and aeration was provided with compressed air from a fish tank aerator at a flow rate of 2 L/min. The final partial pressure of oxygen in the precultures as well as in the fermentors (100–120 Klett units; 1 Klett unit = 10<sup>7</sup> CFU/mL) was typically in the range of 3–7 mbar, a sufficiently low partial pressure of oxygen to permit gratuitous expression of bchl *a*, light-harvesting polypeptides, and RC (Biel & Marrs, 1983; Farchaus et al., 1990, 1992).

Oxygen tension measurements were carried out with a Trioxmatic EO200 Clark-type oxygen electrode connected to an Oxymatic 2000 microprocessor oximeter from WTW GmbH (Weilheim, Germany). The temperature was maintained at 30 °C, and a black cloth was securely wrapped around the fermentor to prevent the admittance of light. This regimen, using a large inoculum and strict adherence to dark chemoheterotrophic conditions, was used to minimize selective pressure for reversion of the engineered mutations or secondary mutations during fermentations required for large-scale purification of mutant RCs. Photoheterotrophic liquid cultures for growth studies were inoculated from late-log-phase chemoheterotrophic cultures to an initial cell density of 2 × 10<sup>8</sup> CFU/mL in SMM supplemented with kanamycin (25 μg/mL). The cultures were maintained at 30 °C in completely filled anaerobic culture tubes (Bellco Glass, Inc., Vineland, NJ) and incubated in darkness for 4–5 h postinoculation before illumination. Illumination was with white light at an intensity of 70–75 W/m<sup>2</sup>. Cell growth was monitored with a Klett–Summerson colorimeter equipped with a Corning No. 66 red filter.

*Escherichia (E.) coli* DH5α (Gibco Laboratories-Bethesda Research Laboratories, Gaithersburg, MD) [F<sup>−</sup> recA1 ϕ80d

lacZΔM15 Δ(lacZYA-argF9)U169 λ<sup>−</sup>] was used as a host strain for all standard cloning steps and plasmid purifications unless specifically stated otherwise. The *E. coli* strain S17-1 (Simon et al., 1983) [recA pro<sup>−</sup> res<sup>−</sup> mod<sup>+</sup> T<sup>p</sup> Sm<sup>r</sup> pRP4-2-TC::Mu-Km::Tn7] used for the conjugative transfer of derivatives of the mob<sup>+</sup> plasmid pRK404 into *R. sphaeroides* was grown in LB medium (Maniatis et al., 1982) supplemented with tetracycline (10 μg/mL) at 37 °C. *E. coli* WK6mutS (Stanssens et al., 1989) [Δ(lac-proAB),galE,stra,muS215::Tn10/F<sup>+</sup>lacI<sup>q</sup>,ZΔM15,proA<sup>+</sup>B<sup>+</sup>] was transformed with derivatives of pMa/c5-8 and used to produce single-stranded DNA from these phasmids with the help of the helper phage M13K07 (Pharmacia P-L Biochemicals Inc., Milwaukee, WI). *E. coli* WK6mutS was grown on M9 minimal medium supplemented with 2 mg/mL vitamin B1 (Maniatis et al., 1982) at 37 °C. Ampicillin (100 μg/mL) or chloramphenicol (40 μg/mL) was added when the strain harbored derivatives of pMa/c. The M13K07 stocks (titer 10<sup>11</sup>–10<sup>12</sup>/mL) used for single-stranded DNA isolations were generated from *E. coli* BMH71-18 [Δ(lac-proAB),thi,supE/F<sup>+</sup>lacI<sup>q</sup>,ZΔM15,proA<sup>+</sup>B<sup>+</sup>] as described by Kramer and Fritz (1987).

**Recombinant DNA Techniques.** The engineered mutations described in this article were generated using the gapped-duplex DNA method developed by Stanssens et al. (1989). The 5.3-kb *HindIII*–*Bam*HI *puf* operon fragment described previously (Farchaus & Oesterheld, 1989) was cloned into the pMa/c5-8 gapped-duplex phasmid system using the corresponding restriction sites located in the polylinker region of these plasmids. The resulting phasmids pMAPLM1 and pMCPLM1 had functional ampicillin and chloramphenicol antibiotic resistance genes, respectively. The gapped-duplex method of generating engineered mutations was chosen for these studies since the entire *puf* operon could be targeted for mutagenesis and only a single subcloning step would be required for introduction of the mutations into *R. sphaeroides*. The only requirement is that unique restriction sites be available at least 100 bp 3' and 5' of the codon targeted for mutation. In this case, unique *Aat*II and *Pvu*II sites 616 bp apart flanked codon L162. A double digestion of pMAPLM1 was carried out with these enzymes under standard conditions, resulting in the generation of a 616-bp *Aat*II/*Pvu*II fragment and a 8487-bp fragment containing the rest of pMa and the *puf* operon insert. The 8.49-kb fragment was separated from the smaller fragment and traces of undigested plasmid by centrifugation at 30 000 rpm and 15 °C in a Kontron TST-41 rotor using sucrose gradients formed in 100 mM NaCl, 100 mM Tris-HCl (pH 8.0), 10 mM EDTA, and 20 μg/mL ethidium bromide. The phasmid pMCPLM1 was packaged as a pseudophage using M13K07. The single-stranded DNA was isolated from the pseudophage using the method described previously (Kramer & Fritz, 1987). A 10-fold molar excess of the purified single-strand pMCPLM1 was combined with the 8.49-kb *Pvu*II/*Aat*II fragment.

Gapped-duplex DNA was formed essentially as described by Stanssens et al. (1989) by heating the mixture to 100 °C for 5 min and further annealing the coding strand from the denatured double-stranded *Pvu*II/*Aat*II fragment to the noncoding single-stranded DNA from pMCPLM1 at 65 °C for a minimum of 10 min. The resulting gapped-duplex DNA had a 616-bp gap, leaving codon L162 exposed as single-stranded DNA for the eventual hybridization with mutagenic oligonucleotides. 21-mer synthetic oligonucleotides corresponding to the coding strand sequence 5'-AACACGGGC-TACACCTACGGC-3' were synthesized on an Applied Biosystems 381A DNA synthesizer and phosphorylated. The codon corresponding to L162Y (shown in bold print and

underlined) was changed using *R. sphaeroides* codon preferences (Williams et al., 1986) to F(TTC), M(ATG), S(TCG), L(CTG), or G(GGC). The oligonucleotides were added to the gapped-duplex *puf* operon DNA in a molar excess of  $\geq 20:1$ , annealed to the gapped region for 5 min at 65 °C, and then held at room temperature for an additional 10 min. Single-stranded DNA regions were then filled in using Klenow DNA polymerase and finally ligated with T4 DNA ligase to create closed covalent circular plasmid DNA. The mismatch-deficient *E. coli* strain WK6mutS was transformed with this DNA using the CaCl<sub>2</sub> method described previously (Maniatis et al., 1982), but with a modification that omitted the 12–24-h incubation step at 4 °C. The transformed WK6mutS was added to LB medium, allowed to express the intact ampicillin resistance gene, and then subjected to ampicillin (100 µg/mL) selective pressure overnight. Plasmid DNA was isolated from the resulting culture using the alkaline lysis miniprep method (Birnboim et al., 1979). WK6mutS was then transformed a second time with the miniprep DNA and plated out on LB plates containing ampicillin (100 µg/mL).

Typically, 100 transformants were then picked and screened using colony hybridizations to distinguish between WT background and mutants. Prehybridization of the colony hybridization nitrocellulose filters was carried out for 2 h at 40 °C in 5× SSPE containing 100 µg/mL sonicated calf thymus DNA (SERVA, Heidelberg, Germany) and 0.3% (w/v) SDS. Hybridizations were carried out with polynucleotide kinase <sup>32</sup>P-5'-labeled aliquots of the same oligonucleotides used to create the mutations originally. A total of 1–2 µCi (1–1.5 pmol) of labeled oligonucleotide was added to the prehybridized filters and allowed to hybridize at 40 °C overnight in 5× SSPE containing 0.3% (w/v) SDS. The 40 °C temperature chosen for the initial annealing permitted hybridization with all colonies whether mutant or WT. By simply washing the filters with increasingly stringent temperatures, the oligonucleotide was removed from WT colonies, leaving the oligonucleotide hybridized with those colonies harboring the desired mutation. Between two and four possible mutants were picked from the colony plates, and single-stranded DNA was isolated from the clones using M13K07 as described above. The mutations at L162 were confirmed by dideoxy sequencing.

Before we proceeded with the characterization of the mutants, the entire 616-bp region was sequenced for both isolates of each mutant to confirm that the only genetic change was the desired engineered alteration at L162. The entire *Bam*HI/*Hind*III *puf* fragment isolated from separate confirmed mutants for each substitution was then subcloned into pRK404. The pRK404 derivatives harboring the mutations were then transformed into *E. coli* S17-1, and the plasmids were conjugally transferred individually into *R. sphaeroides* PUFΔLMX21/3 using the diparental filter-mating procedure described previously (Davis et al., 1988). The pRK404 derivative plasmids were then isolated using an alkaline lysis protocol from selected PUFΔLMX21/3 isolates grown chemoheterotrophically in SMM supplemented with 10% (v/v) LB and 0.2% (w/v) casamino acids (Difco, Detroit, MI). The mutations were then confirmed in the pRK404 derivatives using dot blot hybridizations with the original oligonucleotides used to engineer the mutations. The isolated plasmids were transformed into *E. coli* DH5α. The plasmids were isolated from these transformants, and the 616-bp region between the *Pvu*II and *Aat*II sites in the L162F and L162L mutations was sequenced using the NaOH denaturation double-strand sequencing method (Chen & Seeburg, 1985), confirming that the initial mutations were intact and that no second site mutations had occurred within this region.

The conditions used for restriction endonucleases, T4 DNA ligase, T4 polynucleotides kinase, and *E. coli* DNA polymerase I (Klenow fragment) were as described by the supplier (Boehringer Mannheim, Mannheim, Germany). Dideoxy sequencing was carried out using the Sequenase kit (USB, Cleveland, OH). Plasmid DNA was purified using Qiagen columns as described by the manufacturer (Diagen GmbH, Düsseldorf, Germany). Other standard molecular biological protocols not specifically addressed were as described previously (Maniatis et al., 1982).

**Protein Purification Techniques.** *R. sphaeroides* PUFΔLMX21/3 strains harboring mutations at L162 on the plasmid pRK404 were fermented in 10-L cultures as outlined above. The cells were harvested at 100–120 Klett units by centrifugation in a Stock centrifuge at 6000g for 40 min. The yield of cells was typically 35–40 g of wet weight/10 L. The cell pellet was resuspended in approximately 120 mL of 20 mM Tris-HCl (pH 8.0), frozen in liquid nitrogen in darkness, and stored at –20 °C. The frozen cell pellets were defrosted and stirred for 1 h at room temperature in the presence of a spatula tip of lysozyme and DNase I (Boehringer Mannheim, Mannheim, Germany). The cells were then passed through a French Press cell (Aminco, Lorch, Germany) at 1200 lbs/in<sup>2</sup> (40 000 psi internal pressure) two or three times at 4 °C. Cell debris and unbroken cells were removed by centrifugation at 12000g in an SS-34 rotor at 4 °C for 20 min. The intracellular membranes in the supernatant were pelleted by centrifugation for 2 h at 4 °C and 150000g in a Ti-70 rotor. The intracellular membranes were homogenized and finally diluted with 20 mM Tris-HCl (pH 8.0) to a final concentration of  $A_{870nm} = 50$ . The RCs were extracted by a modified version of the sequential extraction method described previously (Ogrodnik et al., 1988a). The membranes were resuspended in 20 mM Tris-HCl (pH 8.0), 125 mM NaCl, and 1 mM sodium ascorbate at 4 °C in total darkness, and LDAO (Fluka Chemie, Neu-Ulm, Germany), which was first incubated with catalase (1 µg/mL) for a minimum of 24 h to remove traces of peroxides, was added slowly to a final concentration of 0.25% (w/v). The membranes were stirred for 45 min, and nonsolubilized material was pelleted by centrifugation at 150000g for 2 h. The supernatant from the first extraction was enriched in light-harvesting complex II, but contained no detectable traces of photoactive RCs. The pellet was resuspended to its initial volume, and the extraction was repeated a second time with the same detergent concentration. The supernatant from this second extract was enriched in solubilized photoactive RCs. The RC extract was then diluted 1:1 with 20 mM Tris-HCl (pH 8.0) and 0.25% (w/v) LDAO and loaded onto a DEAE 52-cellulose column [preequilibrated with 20 mM Tris-HCl (pH 8.0)] (Whatman, Kent, England) that had a total column volume equivalent to the volume of extract loaded. The column was washed with at least 10 column volumes of 20 mM Tris-HCl (pH 8.0), 80 mM NaCl, and 0.08% (w/v) LDAO. The column was then developed in steps with the same buffer, but with the NaCl increased first to 110 mM and finally to 140 mM. The RC was eluted with the same buffer with 200 mM NaCl and dialyzed overnight against 10 vol of 20 mM Tris-HCl. The remaining light-harvesting complex II contamination was removed on a 0.5 × 20 cm Fractogel TSK DEAE 650 column preequilibrated in 20 mM Tris-HCl (pH 8.0) (Merck GmbH, Darmstadt, Germany). The RC was eluted from this column in 20 mM Tris-HCl (pH 8.0), 160 mM NaCl, and 0.08% (w/v) LDAO. The ratio of the absorbance at 280/803 nm was between 1.1 and 1.4 for all RC preparations used in this and the following studies.

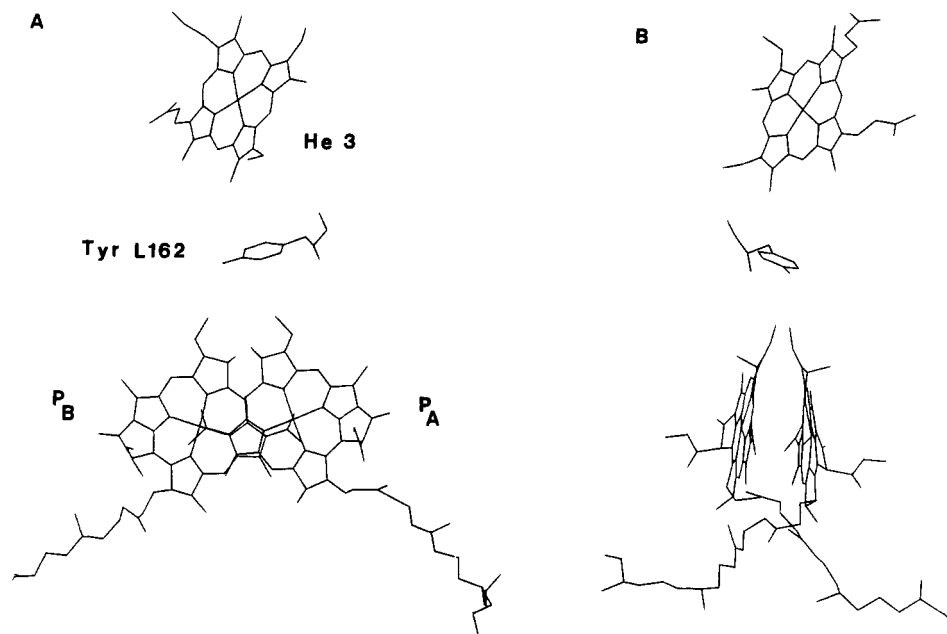


FIGURE 1: Structure of the RC protein of *Rps. viridis* revealing the location of L162Y 6 Å from the edge of the heme and 6 Å from the nearest edge of the bchl dimer forming the special pair (P). Only the heme closest to P is shown, and the phytyl chains of the bchl *a* molecules have been partially deleted. The special pair is viewed from the front (A) and the side (B).

Photobleaching assays in the absence of added quinone revealed that more than 95% of the RCs had a quinone bound to the  $Q_A$  site.

**Spectroscopy.** Measurements of the photobleaching of the  $Q_Y$  region of the RC spectrum in intracellular membranes or with isolated protein were carried out using a photodiode array spectrophotometer (Uhl et al., 1985). The intensity of the measuring beam, which also served as the actinic source, was reduced with a 1% transmittance neutral density filter and was defined spectrally by an RG-665 filter (Schott, Mainz, Germany). The same instrument was used for the cyt *c* turnover assays, which were carried out as described previously (Paddock et al., 1988; Okamura et al., 1982).

**Flash Kinetic Measurements.** The *R. sphaeroides* PUFΔLMX21/3 cells harboring the mutations on pRK404 derivatives were grown chemoheterotrophically in complete darkness in SMM supplemented with tetracycline and kanamycin as described above. Cells were harvested at 67–100 Klett units, washed one time with SMM, and finally suspended to a final volume of 2.2 mL in the same medium supplemented with 10% (w/v) Ficoll 400, 1 mM sodium ascorbate, and 50  $\mu$ M *N,N,N',N'*-tetramethyl-*p*-phenylenediamine (TMPD) (Sigma, München, Germany) to a final cell density of  $7.5 \times 10^9$  CFU/mL. The succinate in the SMM and the added ascorbate/TMPD pair served to keep the cyt *c*<sub>2</sub> in the intact cells in the reduced state. The addition of cyanide or other oxidase inhibitors was found to be unnecessary under the conditions used here.

The sample was situated in a 3 mm thick cuvette which was at 45° to the mutually perpendicular excitation and measuring light beams. Excitation was provided by a short laser pulse (about 10 ns; broad band around 595 nm; energy  $\approx$  2 mJ) at a repetition rate of 0.1 Hz. The pulse was attenuated and homogenized by a piece of ground glass, located at a distance of 65 mm from the cuvette. The measuring beam, provided by a 600-W tungsten lamp, was filtered before the cuvette by a broad-band interference filter ( $\Delta\lambda$  = 160 nm, centered at 1250 nm) and a Schott RG1000 2-mm filter. After passing through the cuvette, the measuring beam was confined by an identical set of filters and focused onto a germanium photodiode (diameter, 3 mm), the output of which was directly

connected (with a 100- $\Omega$  load resistor) to a Tektronix 7912 digitizer equipped with a 1-MHz amplifier. For slower measurements, the photodiode signal was amplified ( $\Delta f$  = 1 Hz to 0.1 MHz) and then measured with a Tracor TN1710 averager. The data presented are the averaged effect of 10–40 individual experiments.

**Materials.** [ $\gamma$ -<sup>32</sup>P]dATP (5000 Ci/mmol) and [ $\alpha$ -<sup>35</sup>S]dATP (>1000 Ci/mmol) were obtained from Amersham (Braunschweig, Germany). Nitrocellulose paper for dot blots was obtained from Schleicher and Schuell (Dassel, Germany). Antibiotics and other chemicals not specified elsewhere were from either Sigma (München, Germany), Riedel-deHäen (Seelze, Germany), or Merck (Darmstadt, Germany).

## RESULTS

Analysis of  $P^+$  rereduction in *R. sphaeroides* by cyt *c*<sub>2</sub> led to the development of a kinetic model requiring complex interactions of the cyt with the RC surface. Although cross-linking and immunological studies (Rosen & Feher, 1983) have provided some clues to the location of the cyt *c*<sub>2</sub> binding site(s) on a rough scale, the molecular details required for optimal binding and donation of an electron to  $P^+$  remained opaque. With the crystallization of the RC from *Rps. viridis*, which included the tetraheme cyt tightly associated with this RC *in vivo*, it was possible for the first time to visualize the protein environment which supports the intraprotein electron-transfer process from heme to  $P^+$ . Analysis of the RC region between the proximal heme and special pair revealed the striking positioning of tyrosine residue L162 halfway between the two chromophores with the edge of the aromatic ring positioned 6 Å from the nearest edge of P and the proximal heme, respectively (Figure 1). The intriguing location of L162Y and the absolute conservation of this residue in all RCs sequenced to date (Williams et al., 1983; Youvan et al., 1984; Shiozawa et al., 1989) led Michel et al. (1986a) to postulate that the residue might play a key role in facilitating the electron transfer between these two components.

With the subsequent crystallization of the RC from *R. sphaeroides* and computer modeling capabilities, it became possible to explore possible binding interactions between cyt *c*<sub>2</sub> and the RC. Two simulations of cyt *c*<sub>2</sub> docking made it

apparent that more than one possibility existed and increased interest in the possible role of L162Y, since one model placed it in a position comparable to that observed in *Rps. viridis* (Allen et al., 1987), while the other placed it off to the side of the M-polypeptide where a role in interprotein transfer was not immediately apparent (Tiede & Chang, 1988). It was our intent to investigate the role of this residue using site-directed mutagenesis first in *R. sphaeroides* and ultimately in *Rps. viridis* (Laussermair & Oesterhelt, 1992).

In order to apply site-directed mutagenesis, the gapped-duplex method (Stanssens et al., 1989) was utilized with the entire 5.3-kb *Bam*HI/*Hind*III *puf* operon shuttle fragment (Farchaus & Oesterhelt, 1989) subcloned into the pMA/C mutagenesis vectors. It was thus possible to engineer mutations into structural genes for the RC L- (*pufL*) or M-subunits (*pufM*) or any of the three other structural genes or the functional oxygen-regulated promoter (Farchaus et al., 1992) harbored on this fragment without further subcloning. DNA sequences were obtained for the WT L162Y (codon TAC) and five site-directed mutants, L162F (TTC), L162S (TCG), L162L (CTG), L162M (ATG), and L162G (GGC), obtained from plasmid isolated from *E. coli* after selection using colony screening. The sequenced region for WT and each mutant included the entire gapped-duplex region (see Materials and Methods) used to generate the mutations and extended several hundred bases beyond. In each case, no mutations other than the desired engineered changes were found. This confirmed the observations of Stanssens et al. (1989) that mutational events outside of the gapped region occur at the very low spontaneous mutation frequency seen for cloned material in the *E. coli* strains, in this case DH5 $\alpha$  and WK6mutS. It should be noted that the complete resequencing for the WT genes isolated here from *R. sphaeroides* ATCC 17023 was also carried out prior to mutagenesis and was deemed necessary as the published sequence for the *pufL* gene was from another strain: *R. sphaeroides* 2.4.1. Although ATCC 17023 was distinct from 2.4.1 (S. Kaplan, personal communication), no differences from the published sequence (Williams et al., 1988) were observed.

Each of the 5.3-kb *Bam*HI/*Hind*III *puf* fragments harboring the mutations shown was then subcloned into the mobilizable low copy number plasmid pRK404 and mobilized into the *R. sphaeroides* *pufLMX* deletion strain described previously (Farchaus & Oesterhelt, 1989). The plasmid harboring the mutated form of the *puf* operon was purified from chemoheterotrophic cultures of each isolate and probed with the oligonucleotide used to introduce the mutation originally. The specific hybridization of each oligonucleotide with the plasmid isolated from each *R. sphaeroides* mutant harboring the corresponding engineered mutation shown in Figure 2 demonstrated that the mutations were stably maintained in the *R. sphaeroides* host under the growth conditions employed. The specificity of the hybridization shown in Figure 2 and the stability of the L162F and L162L mutations were again confirmed at the completion of the experiments described herein by resequencing the region of the *puf* operon originally sequenced. No deviations from the original sequence obtained from plasmids isolated from the earlier *E. coli* steps were observed.

Characterization of generation times under chemoheterotrophic culture conditions where the engineered mutations would be phenotypically silent gave the expected result that mutants and WT had identical generation times of 5.8 h. Growth studies using photoheterotrophic conditions ( $I = 70\text{--}75\text{ W/m}^2$ ) where energy-transfer-related phenomena would not initially be limiting revealed that all were photosynthet-

## Amino acid substitution for codon L 162

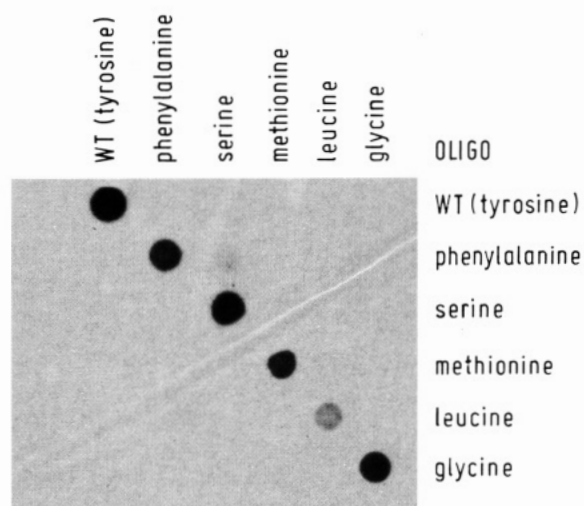


FIGURE 2: Dot blot analysis of the plasmid pRK404 derivatives harboring the engineered mutations isolated from *R. sphaeroides* PUF $\Delta$ LMX21/3. The plasmids were isolated using the alkaline lysis method described in Materials and Methods. Plasmid purity was assessed spectroscopically and confirmed using agarose electrophoresis. One microgram of each plasmid was loaded onto the nitrocellulose. Initial hybridization was at 40 °C. Washes were carried out beginning at 40 °C, after which the temperature was increased by 5 °C increments per wash. The blots were exposed to X-ray film after each wash. The final data shown represent a composite of nitrocellulose strips after various wash temperatures which proved optimal for the individual oligonucleotides. Other conditions were as described in Materials and Methods.

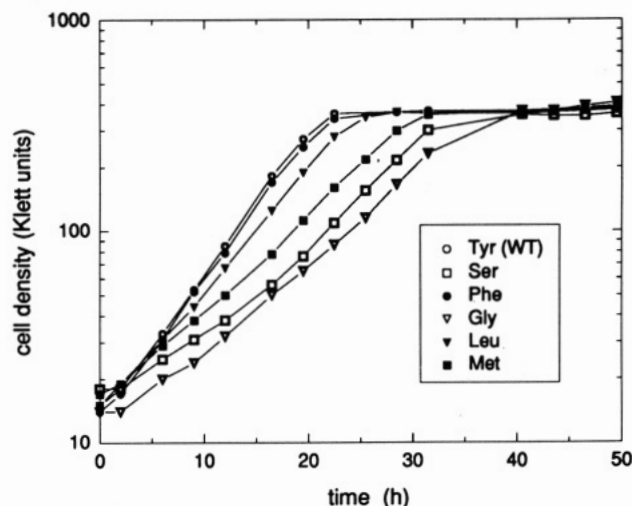


FIGURE 3: Photoheterotrophic growth curves of L162 mutants. Early stationary chemoheterotrophically grown precultures were used as the inoculum at an initial cell density of 14–17 Klett units. No growth was measured during the preincubation period prior to illumination. Illumination was provided by incandescent white light having an incident intensity of 70–75 W/m<sup>2</sup>.

ically competent (Figure 3); however, only L162F and L162L demonstrated generation times similar to that of the WT. The relative order of photosynthetic impairment was L162G ( $t_d$  7.1 h)  $\geq$  L162S ( $t_d$  7.0 h)  $>$  L162M ( $t_d$  6.6 h)  $>$  L162L ( $t_d$  5.1 h)  $\geq$  L162F ( $t_d$  4.3 h) = WT ( $t_d$  4.3 h). Since both L162G and L162S had 65% longer generation times than WT, the lag of 2–4 h seen prior to the onset of growth was attributed to decreased photosynthetic competence. Further studies using photosynthetically grown cells as inoculum revealed that under the same conditions neither lag nor generation time changed. As a final check, CFUs for L162G and L162S were compared



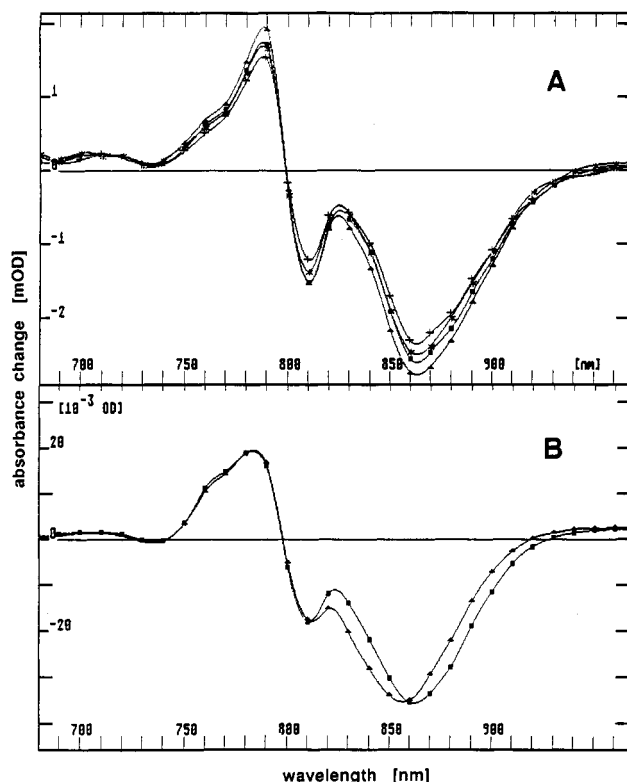


FIGURE 4: Photobleaching of intracytoplasmic membranes (A) and isolated RCs (B) measured for WT L162Y (■) and for L162G (▲), L162F (\*), and L162M (+) mutants. The signal was measured as the difference between an initial spectrum recorded in darkness and a second spectrum 63 ms after the measuring beam was turned on, which also served as the actinic light source. (A) Intracytoplasmic membranes were adjusted to a final concentration of 21.5  $\mu\text{g}$  of membrane protein/mL in 40  $\mu\text{M}$  UHDBT, 10  $\mu\text{M}$  antimycin A, 5  $\mu\text{M}$  valinomycin, 2  $\mu\text{M}$  gramicidin, 5  $\mu\text{M}$   $\text{Fe}(\text{CN})_6^{3-}$ , 50  $\mu\text{M}$   $\text{Fe}(\text{CN})_6^{4-}$ , 50 mM MOPS buffer (pH 7.0), and 100 mM KCl. (B) Isolated RCs in 20 mM Tris-HCl (pH 8.0) and 0.08% (v/v) LDAO; the final RC concentration was 1  $\mu\text{M}$ . The irradiance of the measuring beam used bleached approximately 20% of the RCs.

by plating equal inoculum volumes on SMM plates incubated under chemoheterotrophic and photoheterotrophic conditions. Since equal CFUs were found under both conditions and subculturing did not reveal altered growth parameters in liquid culture, it was concluded that the mutations L162G and L162S were photosynthetically competent, but impaired.

One plausible explanation for the increased generation times observed for L162G and L162S was decreased expression of the mutant RC or decreased structural or photochemical stability induced by the site-directed mutations. To rule this out, the amount of photoactive RC was quantitated using photobleaching assays. The results using isolated intracytoplasmic membranes are shown in Figure 4A. The amounts of photoactive RC were found to be similar for all of the mutants and comparable to levels seen in the WT controls within experimental variation of  $\pm 10\%$ . The bleaching of the  $Q_Y$  transition of the bchl  $a$  dimer had an absorption maximum at 866 nm in the WT and mutants. The intraprotein electrochromic shift of the accessory bchl  $a$  absorption induced in the charge-separated RC was also identical in each case. This was especially critical given that L162Y was located within 6 Å of the special pair, and major disruptions of the overall secondary structure in this region might impact on the absorption characteristics of the bchl  $a$  dimer.

Figure 4B shows the same photobleaching assay performed with isolated RCs. In the presence of 0.025% (v/v) LDAO, there was a hypsochromic shift of the bchl  $a$  dimer  $Q_Y$  absorption maximum for all mutants from the WT value of

866 to 857–860 nm. The shift, which was also observed for WT at higher detergent concentrations ( $\geq 0.25\%$  LDAO), suggested that the removal of L162Y resulted in an increased sensitivity to LDAO-induced structural perturbations in the RCs, although the magnitude of the shift was not found to depend on the engineered residue occupying L162 (Wachtveitl et al., 1993). Such hypsochromic shifts could reflect an increase in the spacing of the bchl components of the bchl dimer (Warshel & Parson, 1987), but the nature of the perturbations within the protein remained unclear. With this result in mind, we took care during the purification to avoid exposing the isolated mutated RCs to excess detergent (see Materials and Methods), and when possible, measurements were made in the absence of detergent. The hypsochromic shift of the bchl  $a$  dimer  $Q_Y$  absorption maxima in the mutants disappeared after LDAO was replaced with 0.8% OG by a detergent exchange method described in Gray et al. (1990). Intra- and interprotein electron-transfer kinetics were measured under both conditions (J. Wachtveitl and P. Mathis, data not shown), and no detergent dependence was observed.

Since it was not known whether the detergent-induced shift reflected large or small perturbations in the RC structure, it was of interest to examine the various intraprotein electron-transfer steps in addition to the interprotein transfer between cyt  $c_2$  and RC. The picosecond kinetics for the primary electron transfer from P to bphe and from bphe to  $Q_A$  were determined for each of the mutants. In the WT RC, the transient absorbance changes recorded at 785 nm were best fit with three time constants (0.9, 3.5, and 200 ps) as reported previously (Holzapfel et al., 1989). The mutants were found to have kinetics which were comparable to those of WT, indicating that the perturbations in structure which shifted the spectrum were not sufficient to affect forward electron-transfer rates. Measurements of the back-reaction kinetics in mutant RCs from  $Q_B^-$  to  $P^+$  (ca. 1 s) (Clayton & Yau, 1972) and  $Q_A^-$  to  $P^+$  (ca. 100 ms) (Kleinfeld et al., 1984) yielded results identical to those found for WT RCs.

Since RC amounts and intraprotein electron-transfer rates were not affected in the mutants, the decreased growth observed under photoheterotrophic conditions could then be the result of an impairment in quinone turnover or in the cytochrome-mediated rereduction of the photooxidized bchl dimer. The cyt  $c$  turnover assay described previously (Paddock et al., 1988) was utilized since it provides information about the apparent ability to doubly reduce  $Q_B$ , the associated protonation steps, and the ultimate release and rebinding of ubiquinone to the  $Q_B$  site. In addition, the assay yielded data on the relative effectiveness of donation of an electron from cyt to the bchl dimer under conditions employing excess cyt. The data shown in Figure 5 demonstrated that the WT RC had a turnover rate of 200 cyt (RC) $^{-1}$  s $^{-1}$ , a value which agreed well with previous reports (Paddock et al., 1988; Gray et al., 1990). The result for L162L was 185 cyt (RC) $^{-1}$  s $^{-1}$ , a value similar to that observed for the WT within experimental error, while the rate of 245 cyt (RC) $^{-1}$  s $^{-1}$  obtained for L162G was slightly faster than that of WT.

The data suggest that there is no impairment in  $Q_B$  turnover and that reduced cyt can still donate to the photooxidized bchl dimer on a time scale which is kinetically faster than the rate-limiting  $Q_B$  release step of RC turnover ( $t_{1/2} = 5$  ms; Debus et al., 1985). Although these data clearly demonstrate that the reduced cyt could still donate to the RC, the assay was carried out with a large excess of cyt, and as such, impaired electron donation from cyt  $c_2$  to  $P^+$ , or impaired binding of the cyt to the RC, would not be apparent. It should also be pointed out that the interaction between mammalian cyt  $c$

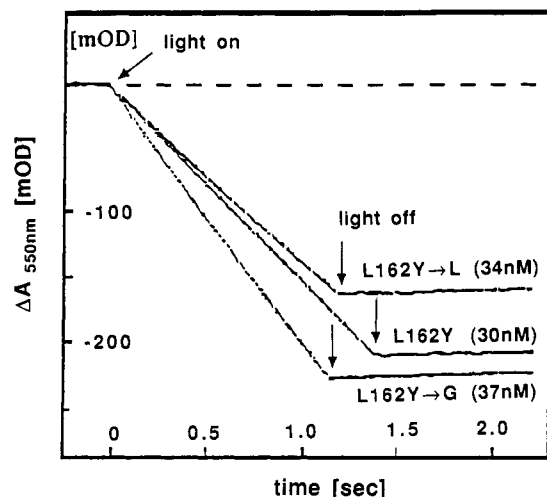


FIGURE 5: Determination of the rate of cyt *c* oxidation by isolated RCs. The RCs were suspended in 1 mM UQ<sub>0</sub>, 20 μM cyt *c* (horse heart) in 10 mM PIPES (pH 6.8), and 0.025% (v/v) LDAO;  $\lambda_{\text{exc}} > 580$  nm and  $\lambda_{\text{det}} = 550$  nm.

and the RC seems to differ markedly from that of the physiological donor cyt *c*<sub>2</sub> and the RC (Tiede, 1987; J. Wachtveitl, unpublished results).

The rereduction kinetics of the bchl dimer can be monitored using the IR absorption peak of the P<sup>+</sup> band (1250 nm), which fortuitously has a wavelength maximum at which no other pigments absorb. With this method and low pO<sub>2</sub> chemoheterotrophically grown cells, which gratuitously express RC and the light-harvesting apparatus, it was possible to analyze the P<sup>+</sup> rereduction kinetics *in vivo*. Since all of the mutant RCs were expressed in the identical *R. sphaeroides* PUFΔLMX21/3 strain and grown under identical conditions, a direct comparison of the IR kinetics of P<sup>+</sup> rereduction in intact cells by the endogenous donor cyt *c*<sub>2</sub> was possible. This allowed the examination of the kinetic efficiency of the donation process in the absence of possible detergent artifacts. Figure 6 shows the results of kinetic measurements of the WT and L162F, L162L, and L162G mutants obtained directly from living chemoheterotrophically grown cultures. Direct analysis from actively growing cultures was found to be critical since freezing cultures disrupted the fast phase of cyt *c*<sub>2</sub> electron donation to the WT RC and slowed the overall kinetics (P. Mathis and J. Wachtveitl, unpublished data).

Flash excitation leads to an unresolvable, rapid ( $< 1$  μs) absorbance increase at 1250 nm which was attributed to the photoactivation of P and the subsequent formation of P<sup>+</sup>. As shown in Figure 6 (top panel labeled L162 Tyr), the decay kinetics for the WT cells included three major phases, termed "fast" ( $\Delta A_f = 46\% \Delta A_{\text{tot}}$ ,  $t_{1/2} = 6$  μs), "slow" ( $\Delta A_s = 45\% \Delta A_{\text{tot}}$ ,  $t_{1/2} = 140$  μs), and "very slow" ( $\Delta A_{vs} = 9\% \Delta A_{\text{tot}}$ ,  $t_{1/2} = 25$  ms). In several independent experiments, the fast phase remained reproducible; however, the half-time of the middle phase was variable, with values ranging between 110 and 162 μs. This kinetic behavior was similar to that reported in earlier work (Prince & Dutton, 1975; Overfield et al., 1979), although the fast phase shown here for the WT was a factor of 2 slower than previously reported values. The reason for this discrepancy was unclear, but differences inherent to the strain ATCC 17023 cannot be ruled out, since separate experiments with strain 2.4.1 cells under identical conditions revealed a half-time of 4 μs (P. Mathis, unpublished results).

Identical measurements for each of the mutants revealed that the decay kinetics were dependent on the engineered mutation. In each case, site-directed mutations removing L162Y resulted in a complete loss of the fast phase of the  $\Delta A$

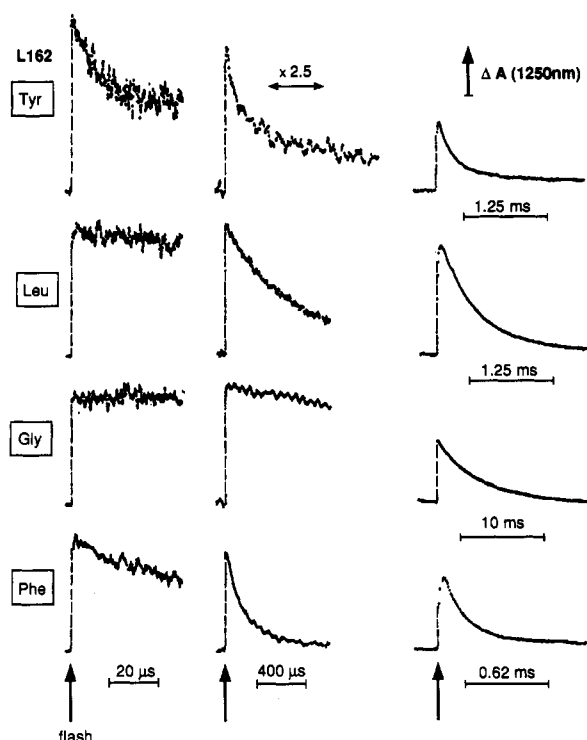


FIGURE 6: Rereduction kinetics of the photooxidized bchl dimer (P<sup>+</sup>) in intact cells. The flash-induced absorption changes were detected at 1250 nm. The excitation wavelength was 595 nm. The traces shown were derived by averaging 10–30 single-flash experiments with a dark adaptation time between individual excitations of 10 s. For the middle column of traces, the horizontal bar corresponds to 400 μs, except for the top trace where it corresponds to 160 μs.

Table I: P<sup>+</sup> Reduction Kinetics of L162 Mutants in Intact *R. sphaeroides* Cells<sup>a</sup>

sample	phase					
	fast (sweep range < 50 μs)		slow (sweep range < 1 ms)		very slow (sweep range < 100 ms)	
	$t_{1/2}$ (μs)	$\Delta A(10^{-4})/\%A_{\text{tot}}$	$t_{1/2}$ (μs)	$\Delta A(10^{-4})/\%A_{\text{tot}}$	$t_{1/2}$ (ms)	$\Delta A(10^{-4})/\%A_{\text{tot}}$
L162Y(WT)	6.0	0.59/46%	140	0.58/45%	25	0.12/9%
L162F	nd	0	95	1.1/93%	25	0.1/7%
L162L	nd	0	420	1.38	0.39	1.24/100%
L162M	nd	0	380	1.24	0.39	1.06/100%
L162S	nd	0	>1000	1.31	3.2	1.4/100%
L162G	nd	0	>1000	1.25	3.4	1.3/100%

<sup>a</sup> Conditions were as described in Figure 6; nd = not detectable.

decay. The kinetics for all of the mutants were apparently monophasic and up to 3 orders of magnitude slower than those in WT cells (Table I). The mutant L162F in which another aromatic, but less polarizable, residue was substituted for L162Y demonstrated the most rapid kinetics of all mutants analyzed. The overall kinetic decay for the L162F mutant was dominated ( $\Delta A = 93\%$ ) by a phase with a half-time of 95 μs. The remaining 7% of the decay was attributable to a very slow phase (Table I). In the L162G and L162S mutants,  $\Delta A$  recovers nearly exponentially with a half-time of 3.4 ms, whereas a similar, although faster, reaction occurs in L162L and L162M ( $t_{1/2} = 390$  μs).

The redox poisoning of the cyt *c*<sub>2</sub> was similar in each case, as P<sup>+</sup> was ultimately rereduced completely. The half-time for this process in even the slowest mutants L162G and L162S was 5–10 times faster than the back-reaction from Q<sub>A</sub><sup>-</sup> or 50–100 times faster than the back-reaction from Q<sub>B</sub><sup>-</sup>, allowing us to rule out contributions from either of these reactions in the decay kinetics shown. Although it was impossible to distinguish between impaired binding or changes in the actual

electron-transfer rate constants from these results, it was nonetheless apparent that the donation of an electron from the reduced cyt  $c_2$  to the photooxidized bchl dimer was impaired in each of the mutants, with the relative order of the impairment being  $G \approx S > L \approx M > F \gg Y$ .

## DISCUSSION

Five site-directed mutants (L162F, L162S, L162L, L162M, and L162G) were engineered by means of the gapped-duplex method (Stanssens et al., 1989) to probe the possible role of L162Y in the cyt  $c_2$  mediated rereduction of  $P^+$  in *R. sphaeroides*. This technique was chosen since it was, in theory, possible to clone and subsequently mutagenize each of the five genes within the 5.3-kb *puf* operon shuttle fragment described previously, while obviating the need for multiple subcloning steps required when other methods were utilized. The mutations introduced into the RC L-subunit (encoded by the *pufL* gene) were confirmed by sequencing the original vectors from *E. coli* and after mobilization into the *R. sphaeroides* host strain PUF $\Delta$ LMX 21/3 (Farchaus & Oesterhelt, 1989) by using dot blots (Figure 2). Although the possibility of secondary mutations outside the sequenced region of *pufL* or *pufM* could not be rigorously ruled out, the probability of such events causing the observed effects was extremely remote since each mutation was engineered in separate experiments. In addition, the WT described in this article was subjected to the same protocol using the same clones and plasmid preparations which were used repetitively to create the mutants. All of the *R. sphaeroides* isolates used here and in the following article were cultured and maintained using dark chemoheterotrophic conditions required to minimize selective pressure for reversion or secondary mutations.

Comparison of the generation times for each of the mutants described here under chemoheterotrophic and photoheterotrophic conditions revealed that all of the mutants were indistinguishable from WT under chemoheterotrophic conditions and that all were photosynthetically competent. This is in general agreement with the findings of L162 mutations engineered in *Rhodobacter capsulatus*, with the exception of a single mutant L162K which was photosynthetically incompetent (Jovine et al., 1990). The L162K mutant was not made in *R. sphaeroides*. Two of the mutants described here, L162G and L162S, were found to be photosynthetically competent but impaired, with generation times increased 65% relative to the same deletion strain complemented with WT genes.

Light-minus-dark difference spectroscopy was used to quantitate RCs in isolated intracytoplasmic membranes for each of the mutants (Figure 4A). The amounts of RC expressed and the absorption maxima for the bchl dimer  $Q_Y$  transition and the intraprotein electrochromic shift were comparable to the signals obtained from the WT RC. Since the photobleaching experiments shown in Figure 4A were recorded on the millisecond time scale using light intensities insufficient to bleach  $Q_A$ -free samples, the amplitudes of the spectra were direct measures of the photoactive RC with the  $Q_A$  site occupied and capable of receiving an electron to form the stabilized  $P^+Q_A^-$  or  $P^+Q_B^-$  radical pair states. If, on the other hand, the samples were lacking  $Q_A$  in the isolated membranes, the forward electron transfer would be blocked at the state of the bphe  $a$  anion on the active branch of the RC ( $H_A^-$ ). In the absence of  $Q_A$ , the radical state  $P^+H_A^-$  decays rapidly to the ground state either directly ( $t_{1/2} \approx 10$  ns) or via the triplet state,  $^3PH$  ( $t_{1/2} \approx 100$   $\mu$ s) (Ogrodnik et al., 1988b), and no net signal change would be recorded on the time scale used.

As a first step in further characterization, similar light-minus-dark difference spectra of LDAO-solubilized RCs

(Figure 4B) were carried out. A pronounced hypsochromic shift in the  $Q_Y$  band of the primary donor for all of the mutants, suggestive of a perturbation in the spacing of the two bchl dimer molecules, was found. In spite of this shifted absorption band, the rates of ultrafast forward intraprotein electron transfer were indistinguishable for WT values (Holzapfel et al., 1990). The rates of back-reactions were likewise unaffected in all of the mutants. Primary charge separation and the structural changes in the protein environment of the bchl dimer were not related in the case of L162, although earlier studies showed that mutations introduced on the opposite (cytoplasmic) side of the bchl dimer near the accessory bchl  $a$ , such as in position M210, can affect forward rates (Gray et al., 1990, Finkle et al., 1990, Nagarajan et al., 1990).

The turnover assay in Figure 5 showed a comparable rate of cyt oxidation for all RCs tested, which was in agreement with the measurements performed with *R. capsulatus* L162 mutants (Bylina et al., 1988). These results confirm that the quinol/quinone exchange at the  $Q_B$  site can still occur at a normal rate. However, for several reasons these experiments do not provide information about the  $P^+$  rereduction process *in vivo*. First, cyt  $c$  and cyt  $c_2$  interact quite differently with the RC (Tiede, 1987), and secondly, even a decrease in the electron-transfer rate by 3 orders of magnitude would escape detection by this method. Furthermore, cyt  $c$  is present in large excess over RCs with the experimental design utilized for this type of assay, and an altered dissociation constant or a change in reaction order would not be readily apparent.

Kinetic measurements made at 1250 nm using intact cells, in the absence of added detergent, revealed that the rate of cyt  $c_2$  mediated  $P^+$  rereduction was drastically altered for each of the mutants (Figure 6). The fast phase of  $P^+$  rereduction seen in fresh WT cells under the physiological conditions used here was absent in all of the mutants. In previous studies of WT RCs, this microsecond phase was attributed to a bound and correctly oriented cyt  $c_2$  molecule. Interestingly, the most rapid decay observed for all of the mutants was for the only site-directed change that introduced another aromatic residue, L162F. The decay in this case was dominated (93%) by a component with a half-time of 95  $\mu$ s. All other aliphatic substitutions, whether polar or nonpolar, resulted in largely monophasic kinetics in the hundreds of microseconds (L162L,M) or milliseconds range (L162S,G).

On the basis of the comparative rates of back-reaction from  $Q_B^-$  to  $P^+$  ( $t_{1/2} \approx 1$  s) to  $P^+$  rereduction by cyt  $c_2$  in the mutants (Table I), it was not immediately apparent why the rates of electron transfer shown in Table I would directly result in decreased photoheterotrophic growth. Given that the mutants and WT were expressed equally effectively in the same genetic background and RC function was otherwise unaltered, a probable cause might lie in the interaction between RC and cyt  $c_2$ . Initial EPR measurements of the redox state of the cyt  $c_2$  pool *in vivo* confirmed that cyt  $c_2$  oxidation was impaired in L162G (W. Nitschke and J. Wachtveitl, unpublished observations). This finding might be due to the extremely slow electron-transfer reaction from cyt  $c_2$  to  $P^+$ . A test of cyt  $c_2$  mobility (Wachtveitl et al., 1993) provided evidence for a drastically lower cyt  $c_2$ -RC dissociation rate. Since mobility is of crucial importance for the physiological function of cyt  $c_2$ , which acts as an electron shuttle between the cyt  $b_6$  complex and the RC, slower dissociation could explain the impaired photoheterotrophic growth.

The loss of the rapid kinetic component in the mutants suggested that L162Y plays a role in defining the WT kinetics for  $P^+$  rereduction. A vital role for a surface-exposed tyrosine has been observed for pea plastocyanin (He et al., 1991).



Substitution for this residue resulted in either weaker binding and/or a decreased intrinsic rate of electron transfer and weaker binding. Clearly the results presented here can be explained by changes in docking, reorientation, and/or intrinsic electron-transfer rates. Any or all of these effects may be the result of direct loss of L162Y or indirect effects on the RC structure. Analysis of the refined *Rps. viridis* crystal structure revealed that L162Y is connected to M190S via a water molecule and two H-bonds. The importance of this interpolypeptide bond is evidenced by the high degree of conservation: M188S was found at homologous positions in all sequences on photosynthetic bacteria [M188S in *R. sphaeroides*, Williams et al. (1986); M190S in *Rps. viridis* and *R. capsulatus*, Michel et al. (1986b) and Youvan et al. (1984); and M178S in *C. aurantiacus*, Shiozawa et al. (1989)]. From these results, further work will be required to define the role of this aromatic residue precisely, but drastic changes caused by its removal are consistent with a growing body of evidence from other systems [reviewed in Isied (1984); McLendon & Hake, 1992] in which key roles for aromatic residues have already been explored. In order to distinguish between docking, binding, or electron-transfer roles for this residue, further kinetic analysis was carried out using isolated RCs; this work is described in the accompanying article.

## REFERENCES

- Allen, J. P., Feher, G., Yeates, T. O., Komiya, H., & Rees, D. C. (1987) *Proc. Natl. Acad. Sci. U.S.A.* **84**, 6162–6166.
- Biel, A. J., & Marrs, B. L. (1983) *J. Bacteriol.* **156**, 686–694.
- Birnboim, H. C., & Doly, J. (1979) *Nucleic Acids Res.* **7**, 1513–1523.
- Breton, J., Martin, J. L., Fleming, G. R., & Lambry, J. C. (1988) *Biochemistry* **27**, 8276–8284.
- Bylina, E. J., Jovine, R., & Youvan, D. C. (1988) in *The Photosynthetic Bacterial Reaction Center, Structure and Dynamics* (Breton, J., & Vermeglio, A., Eds.) pp 113–118, Plenum Press, New York.
- Chen, E. J., & Seeburg, P. H. (1985) *DNA* **4**, 165–170.
- Clayton, R. K., & Yau, H. F. (1972) *Biophys. J.* **12**, 867–881.
- Coleman, W. J., & Youvan, D. C. (1990) *Annu. Rev. Biophys. Chem.* **19**, 333–367.
- Davis, J., Donohue, T. J., & Kaplan, S. (1988) *J. Bacteriol.* **170**, 320–329.
- Debus, R. J., Feher, G., & Okamura, M. Y. (1985) *Biochemistry* **24**, 2488–2500.
- Debus, R. J., Barry, B. A., Sithole, I., Babcock, G. T., & McIntosh, L. (1988) *Biochemistry* **27**, 9071–9074.
- Deisenhofer, J., & Michel, H. (1989) *EMBO J.* **8**, 2149–2170.
- Deisenhofer, J., Epp, O., Miki, K., Huber, R., & Michel, H. (1985) *Nature* **318**, 618–624.
- El-Kabbani, O., Chang, C. H., Tiede, D., Norris, J. R., & Schiffer, M. (1991) *Biochemistry* **30**, 5361–5369.
- Farchaus, J. W., & Oesterheld, D. (1989) *EMBO J.* **8**, 47–54.
- Farchaus, J. W., Grünberg, H., & Oesterheld, D. (1990) *J. Bacteriol.* **172**, 977–985.
- Farchaus, J. W., Barz, W. P., Grünberg, H., & Oesterheld, D. (1992) *EMBO J.* **11**, 2779–2788.
- Finkele, U., Lauterwasser, C., Zinth, W., Gray, K. A., & Oesterheld, D. (1990) *Biochemistry* **29**, 8517–8521.
- Gray, K. A., Farchaus, J. W., Wachtveitl, J., Breton, J., & Oesterheld, D. (1990) *EMBO J.* **9**, 2061–2070.
- He, S., Modil, S., Bendall, D. S., & Gray, J. C. (1991) *EMBO J.* **10**, 4011–4016.
- Holzappel, W., Finkele, U., Kaiser, W., Oesterheld, D., Scheer, H., Stolz, H. U., & Zinth, W. (1989) *Chem. Phys. Lett.* **160**, 1–7.
- Holzappel, W., Finkele, U., Kaiser, W., Oesterheld, D., Scheer, H., Stolz, H. U., & Zinth, W. (1990) *Proc. Natl. Acad. Sci. U.S.A.* **87**, 5168–5172.
- Isied, S. S. (1984) *Progr. Inorg. Chem.* **32**, 443–517.
- Jovine, R. V. M., Bylina, E. J., Tiede, D. M., & Youvan, D. C. (1990) *Plant Gene Transfer*, 217–224.
- Kaufmann, K. J., Petty, K. M., Dutton, P. L., & Rentzepis, P. M. (1976) *Biochem. Biophys. Res. Commun.* **70**, 839–845.
- Kleinfeld, D., Okamura, M. Y., & Feher, G. (1984) *Biochim. Biophys. Acta* **766**, 126–140.
- Kramer, W., & Fritz, H. J. (1987) *Methods Enzymol.* **154**, 350–367.
- Laussermair, E., & Oesterheld, D. (1992) *EMBO J.* **11**, 777–783.
- Liang, N., Mauk, A. G., Pielak, G. J., Johnson, J. A., Smith, M., & Hoffman, B. M. (1988) *Science* **240**, 311–313.
- Maniatis, T., Fritsch, E. F., & Sambrook, J. (1982) in *Molecular cloning: A laboratory manual*, Cold Spring Harbor Laboratory Press, Cold Spring Harbor, NY.
- McLendon, G., & Hake, R. (1992) *Chem. Rev.* **92**, 481–490.
- Michel, H., Epp, O., & Deisenhofer, J. (1986a) *EMBO J.* **5**, 2445–2452.
- Michel, H., Weyer, K. A., Grünberg, H., Dunger, I., Oesterheld, D., & Lottspeich, F. (1986b) *EMBO J.* **5**, 1149–1158.
- Nagarajan, V., Parson, W. W., Gaul, D., & Schenck, C. (1990) *Proc. Natl. Acad. Sci. U.S.A.* **87**, 7888–7892.
- Ogrodnik, A., Volk, M., Letterer, R., Feick, R., & Michel-Beyerle, M. E. (1988a) *Biochim. Biophys. Acta* **936**, 361–371.
- Ogrodnik, A., Volk, M., & Michel-Beyerle, M. E. (1988b) in *The Photosynthetic Bacterial Reaction Center, Structure and Dynamics* (Breton, J., & Vermeglio, A., Eds.) pp 177–183, Plenum Press, New York.
- Okamura, M. Y., Debus, R. J., Kleinfeld, D., & Feher, G. (1982) in *Function of Quinones in Energy Conserving Systems* (Trumpower, B. L., Ed.) pp 299–317, Academic Press, New York.
- Overfield, R. E., Wraight, C. A., & DeVault, D. (1979) *FEBS Lett.* **105**, 137–142.
- Paddock, M. L., Rongey, S. H., Abresch, E. C., Feher, G., & Okamura, M. Y. (1988) *Photosynth. Res.* **17**, 75–96.
- Prince, R. C., & Dutton, P. L. (1975) *Biochim. Biophys. Acta* **387**, 609–613.
- Rees, D. C., Komiya, H., Yeates, T. O., Allen, J. P., & Feher, G. (1989) *Annu. Rev. Biochem.* **58**, 607–633.
- Rockley, M. G., Windsor, M. W., Cogdell, R. J., & Parson, W. W. (1975) *Proc. Natl. Acad. Sci. U.S.A.* **72**, 2251–2255.
- Rosen, D., Okamura, M. Y., & Feher, G. (1980) *Biochemistry* **19**, 5687–5692.
- Rosen, D., Okamura, M. Y., Abresch, E. C., Valkirs, G. E., & Feher, G. (1983) *Biochemistry* **22**, 335–341.
- Shiozawa, J. A., Lottspeich, F., Oesterheld, D., & Feick, R. (1989) *Eur. J. Biochem.* **180**, 75–84.
- Simon, R., Priefer, U., & Puehler, A. (1983) *Bio/Technology* **1**, 784–791.
- Sistrom, W. R. (1960) *J. Gen. Microbiol.* **22**, 778–785.
- Stanssens, P., Opsomer, C., McKeown, Y. M., Kramer, W., Zabeau, M., & Fritz, H. J. (1989) *Nucleic Acids Res.* **17**, 4441–4454.
- Tiede, D. M. (1987) *Biochemistry* **26**, 397–410.
- Tiede, D. M., & Chang, C. H. (1988) *Isr. J. Chem.* **28**, 183–191.
- Uhl, R., Meyer, B., & Desel, H. (1985) *J. Biochem. Biophys. Methods* **10**, 35–48.
- Wachtveitl, J., Farchaus, J. W., Mathis, P., & Oesterheld, D. (1993) *Biochemistry* **32**, following article in this issue.
- Warshel, A., & Parson, W. W. (1987) *J. Am. Chem. Soc.* **109**, 6143–6152.
- Williams, J. C., Steiner, L. A., Ogden, R. C., Simon, M. I., & Feher, G. (1983) *Proc. Natl. Acad. Sci. U.S.A.* **80**, 6505–6509.
- Williams, J. C., Steiner, L. A., & Feher, G. (1986) *Proteins* **1**, 312–325.
- Woodbury, N. W., Becker, M., Middendorf, D., & Parson, W. W. (1985) *Biochemistry* **24**, 7516–7521.
- Wraight, C. A. (1979) *Biochim. Biophys. Acta* **548**, 309–327.
- Youvan, D. C., Bylina, E. J., Alberti, M., Begusch, H., & Hearst, J. E. (1984) *Cell* **37**, 949–957.